

Short Communication

Multi-faceted monitoring of powder flow rate variability in directed energy deposition

Felicity S.H.B. Freeman^{a,*}, B Thomas^a, L Chechik^a, Iain Todd^a^a Department of Materials Science & Engineering, University of Sheffield, Sheffield, S1 3JD, UK

ARTICLE INFO

Keywords:

Directed energy deposition
Powder flow rate
Powder flow imaging
Melt pool imaging

ABSTRACT

Powder flow rate is a key parameter in Directed Energy Deposition (DED) processes. During a typical build, if powder flow rate is reduced for just 1 second, 30 mm of melt track is affected. Consequently, even a small variation in powder flow rate can have significant implications on build quality. In this work, the powder flow stability for different types of 316 L steel powders was quantified using a combination of methodologies including offline weight measurements, flow imaging, *in-situ* build data and coaxial melt pool imaging. Flow rate oscillation was observed, correlated with the periodicity of powder hopper turntable rotation, at sufficient magnitude to cause build quality effects and be identifiable in coaxial melt pool imaging. The implications of flow rate variation on the use of melt pool imaging for closed-loop control are discussed.

1. Introduction

Directed Energy Deposition (DED) systems use nozzles to focus a mixed stream of metal powder and gas into the melt pool, making it one of the more critical components affecting build quality[1,2]. Many studies on DED have included powder flow rate as an input variable[3,4], of equal importance with laser power and travel speed, although there is minimal literature quantifying or considering the effect of flow rate variation[5,6]. Flow rate is often measured offline as part of set-up, collecting powder over 1–2 min and then measuring total mass, which will not identify higher frequency variation[7].

Studies have considered how the nozzle design influences the shape of the powder cone, using a range of measurement and modelling techniques to determine the shape and position of the powder focal point compared with the laser focal point[1,2,8]. These have included analysis using line lasers and high speed cameras to understand the shape of the powder flow distribution[9–11], which has led to a commercially available system developed by Fraunhofer IWS[12]. These studies have considered snapshot behaviour from a single image exposure rather than how the flow rate and shape of powder distribution varies over time.

There are a range of different powder hopper designs available; the majority have volumetric control of the powder feed rate, with a mass measurement taken at the nozzle before build. There are some gravimetrically controlled systems available, but the accuracy of these is not yet sufficient for most DED processes (± 2 g/min for Oerlikon Metco Single 220 Series[13])

From literature, powder flow rate is generally between 5 g/min and 20 g/min in DED, although some use flow rates outside this range[14–16]. As the hoppers are volumetrically controlled, the material density and packing density have an influence on the volume of powder required to achieve a target mass flow rate. In the case of 316 L steel, with a solid density of 7.8 g/cm³ and an assumed packing density of 60%, this gives a volumetric flow rate of only 1.5 cm³/min bulk powder[17].

To understand how this can impact the process, it is necessary to consider the distance that a DED nozzle moves relative to any variation in powder flow rate. At a nozzle speed of 2000 mm/min, if mass flow drops for just 1 second it affects 30 mm of melt track, and at higher speeds the affected region will be even longer[15].

Additive manufacturing research is focused on the development of monitoring systems used in conjunction with closed-loop control and machine learning algorithms to continuously monitor build quality and adjust input parameters[15,18–20]. Understanding variation in powder mass flow rate and its effect on the build must be part of that development process. Further, as many of these systems rely on imaging techniques, if powder flow variation affects image brightness then it has implications for the control approach, and could even cause an incorrect control response.

2. Method & materials

The Directed Energy Deposition (DED) machine used in this work was a BeAM Magic 2.0. This has two nozzles; the 24Vx nozzle has a

* Corresponding author at: Department of Materials Science & Engineering, University of Sheffield, Sheffield, S1 3JD, UK.

E-mail address: f.freeman@sheffield.ac.uk (F.S.H.B. Freeman).

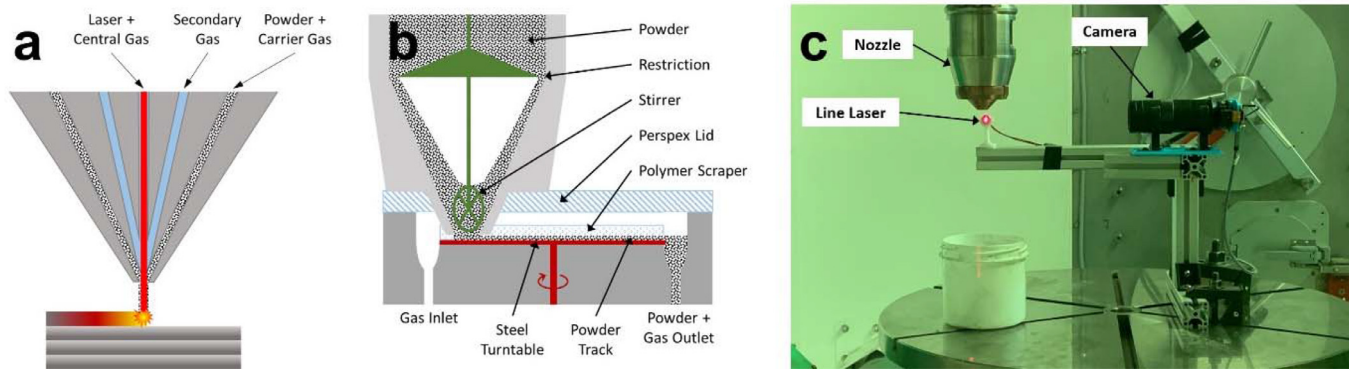


Fig. 1. a) BeAM Magic 2.0 nozzle schematic; b) Medicoat AG disc hopper schematic; c) Set-up for side-view flow imaging using line laser.

Table 1

Size and shape characteristics of gas atomised and water atomised 316 L powder.

	D10 (μm)	D50 (μm)	D90 (μm)	Sphericity	Aspect Ratio
GA316	51.5	69.9	91.4	0.83	0.82
WA316	54.2	77.6	103.9	0.70	0.66

2.25 mm spot diameter and normally requires 16–17 g/min of steel powder, the 10Vx nozzle has a 0.70 mm spot diameter using 6.5–7.5 g/min of steel powder (Fig. 1a). All parameters quoted are the set-points used in the build program, without adjustment for efficiency losses.

The Magic 2.0 is fitted with disc hoppers (Fig. 1b), which store powder in a vertical cylinder. At the base of the cylinder is a restriction, leading down to a funnel and a stirrer. The restriction acts to make the powder in the funnel independent of the pressure from the powder above. From the funnel, powder flows down through a polymer scraper, manufactured from RCH1000, to a steel turntable. The turntable brings the powder to the front of the hopper, where it is mixed with the carrier gas and channelled into pipework leading to the nozzle.

The scraper sets the width and depth of the powder track, which combines with the speed of the turntable to set the powder flow rate. GA316 powder used a low volume scraper, with a powder track 15 mm wide and 0.4 mm high. WA316 powder used a high volume scraper, with a powder track 15 mm wide and 1.2 mm high.

All trials were carried out with 3 l/min carrier gas, 3 l/min central gas and 6 l/min secondary gas, which are the recommended parameters from BeAM. Argon was used for all gas flows.

This study used gas atomised and water atomised 316 L steel powder (Table 1 & Table 2)[21]. The gas atomised powder (GA316) was manufactured by Sandvik, in batch 21D0104. The water atomised powder (WA316) was manufactured by Hogan as in batch 2,782,458.

Offline measurements of powder flow used Kern PCB-2500 scales placed directly below the nozzle, with an empty tub to collect the powder. The scales were connected to a computer via RS232-USB interface, with data logging software recording the mass and associated timestamp at a rate of 3 Hz. This was converted to mass flow rate afterwards.

Flow imaging was carried out using a line-laser and Raspberry Pi camera with a 10x microscope objective placed at 90° to each other (Fig. 1c). The line-laser was aligned vertically and positioned to illuminate the central slice of the powder flow, with the camera detecting the reflected light from the flowing powder. This is similar to the Fraunhofer L1sec system[12], but at an approximate cost of only £100. The camera was connected to a computer via USB, and image collection and processing managed by a Python script.

Cylindrical builds for ‘constructive’ and ‘destructive’ interference were carried out using the 24Vx nozzle, at 800 W and 1000 mm/min. The builds were spiral cylinders, taking 20 rotations to move a vertical distance of 15 mm, corresponding to a layer thickness of 0.75 mm.

The power was increased to 960 W for the first two layers to improve adhesion to the baseplate.

Cylindrical builds for melt pool imaging were carried out using the 10Vx nozzle, at 250 W and 2200 mm/min. The builds were spiral cylinders, taking 150 rotations to move a vertical distance of 30 mm, corresponding to a layer thickness of 0.2 mm.

Melt pool images were captured by a co-axial Basler acA1440-73gm camera, filtered to accept wavelengths in the range 660 – 1000 nm, excluding reflected light from the laser. 12-bit images (500×500 px) were collected from the camera at 28 frames per second with an exposure of 4000 ms. The camera was connected to a computer via Ethernet cable, with image collection and processing managed by a Matlab script.

3. Results

3.1. Hopper flow measurements

Offline measurement was carried out to quantify and analyse powder flow rate instabilities. The primary focus was the frequency of hopper turntable rotation, which is the characteristic of this hopper design most likely to introduce variation.

The hopper was loaded with approximately 3 kg of GA316 powder and >200 g of powder was run through the pipework to allow the system to stabilise before collecting data. The maximum hopper rotation speed is 10 rpm, and data was collected at 0.5, 1.0, 1.5, 2.0, 2.5 and 3.0 rpm, covering the standard range of powder flow rates found in literature[14–16]. The data was collected as a single run, with 5 min at each turntable speed stepping up from 0.5 rpm to 3.0 rpm. The first 30 s at each speed was excluded from the analysis, to remove the effect of overshoot when changing speed[6].

The raw data was noisy, with the magnitude of the noise increasing with flow rate, obscuring underlying patterns (Fig. 2a & Fig. 2b). The highest frequency oscillation, causing low flow measurements regularly every 3 s at all turntable speeds is believed to be a measurement artefact due to buffering in the data transfer between the scales and the computer.

Taking a moving average over 30 data points (Fig. 2c) showed a clear oscillating pattern, where the amplitude and period increased with turntable speed. Taking the moving average over 180 data points (Fig. 2d) damped out the oscillation for all the lower turntable speeds, and significantly reduced the amplitude for the higher speeds.

To confirm that these results were not due to erroneous set-up, the trial was repeated with WA316; a cheaper, less spherical powder. The WA316 powder was set up using a high volume scraper, where the increased track width and depth compensated for the lower sphericity, reducing the risk of the powder clumping as it flowed onto the turntable. This trial was conducted 3 months after the GA316 trial, with different environmental conditions and with approximately 2 kg of powder in the hopper.

Table 2
Chemistry of gas atomised and water atomised 316 L powder.

	C wt%	Co wt%	Cr wt%	Cu wt%	Fe wt%	Mn wt%	Mo wt%	Nb wt%	Ni wt%	P wt%	Si wt%	V wt%	W wt%	O ppm
GA316	0.018	0.07	16.82	0.17	Bal	1.58	2.22	0.03	10.40	0.024	0.97	0.05	0.02	409
WA316	0.026	0.05	16.97	0.05	Bal	0.10	2.34	<0.02	12.76	0.013	0.84	0.05	<0.02	2336

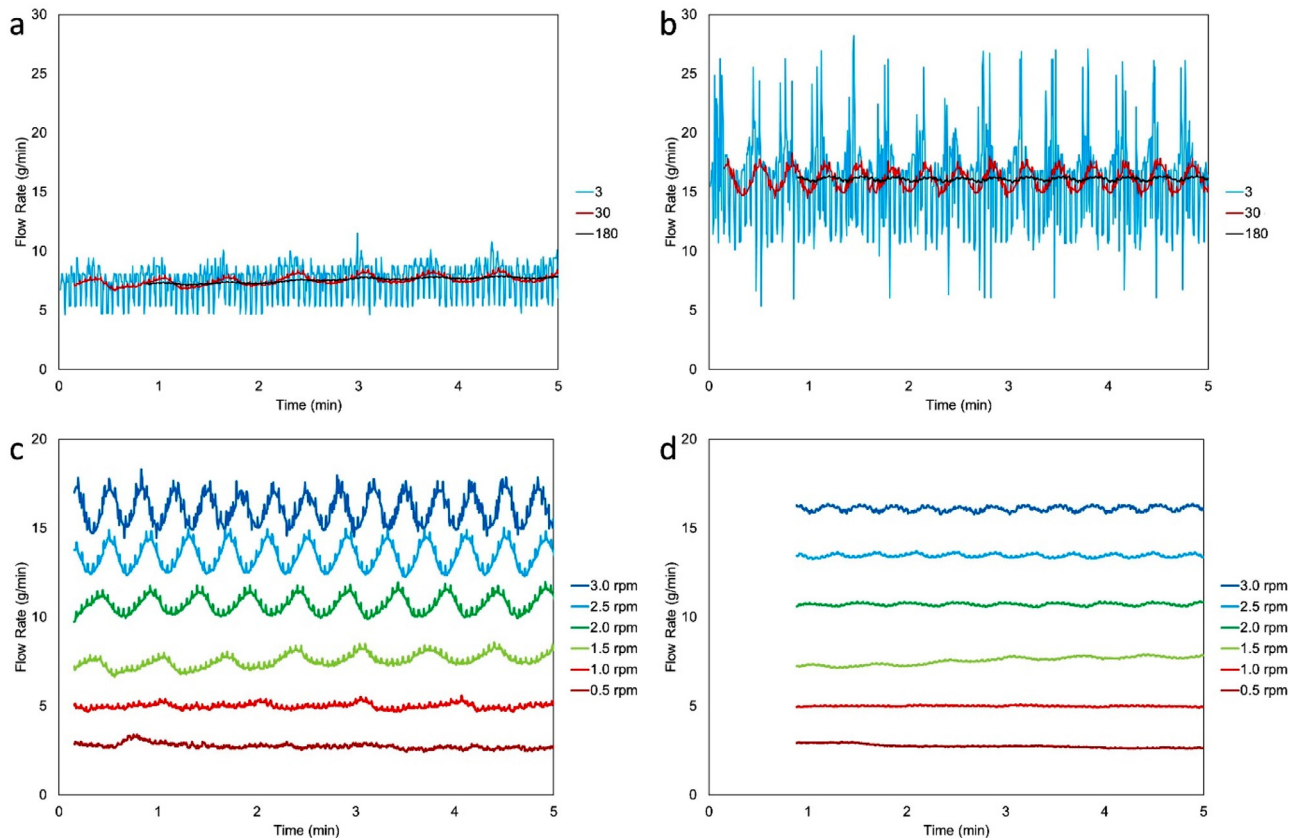


Fig. 2. Gas atomised 316 L with low volume scraper. a) Mass flow rate at 1.5 rpm turntable speed, moving average window over 3 data points (1 second), 30 data points (10 s) and 180 data points (60 s); b) Mass flow rate at 3.0 rpm, moving average window over 3 data points (1 second), 30 data points (10 s) and 180 data points (60 s); c) Moving average window over 30 data points for all turntable speeds; d) Moving average window over 180 data points for all turntable speeds.

Table 3

Flow behaviour of GA316 and WA316 at matched turntable speeds and at matched flow rates.

	At 3 rpm Averageg/min	StDevg/min	At ≈ 11 g/min Averageg/min	StDevg/min
GA316	16.1	3.6	10.7	1.9
WA316	34.8	8.5	11.7	4.8

With the high volume scraper, the WA316 achieved higher average flow rates than the GA316 for the same turntable speed, but the data was noisier, potentially due to the less spherical powder flowing less evenly (Fig. 3& Table 3). The high frequency noise is again believed to be a measurement artefact from data transfer buffering between the scales and the computer.

Filtering the WA316 data taken at 2 rpm shows an underlying oscillation (Fig. 4a). The match to the turntable speed is generally good, except for a shift around 3 min into the data capture, potentially suggesting an additional unidentified source of flow variation. Filtered data taken at 3 rpm also shows oscillation, and with larger amplitude than at 2 rpm, consistent with the behaviour of the GA316 trial (Fig. 4b). For

the data at 3 rpm, after filtering to remove the noise, the flow rate was 35.3 ± 0.5 g/min, a lower magnitude of oscillation than for GA316 at the same turntable speed.

3.2. Nozzle imaging

Nozzle flow imaging was carried out to confirm the variation in flow rate identified by offline weight measurement. This used the 24Vx nozzle with a nominal mass flow rate of 16.5 g/min, requiring a turntable speed of 3.1 rpm for GA316 powder with this hopper set up.

A series of 32 greyscale images were taken, evenly spaced across a full turntable rotation. Where the powder flow was denser, more of the line-laser was reflected into the camera, giving a brighter image. After background subtraction, the sum of all 8-bit pixel values for each image showed an oscillatory pattern very similar to that observed in the mass flow measurements (Fig. 5a).

Superimposing false-colour on the individual images for the lowest and highest readings from repeat T1 (Fig. 5b & Fig. 5c) shows that this oscillation is driven by changes within the powder stream. Image #19, taken at the peak of the oscillation, had a much brighter, denser powder stream than Image #5.

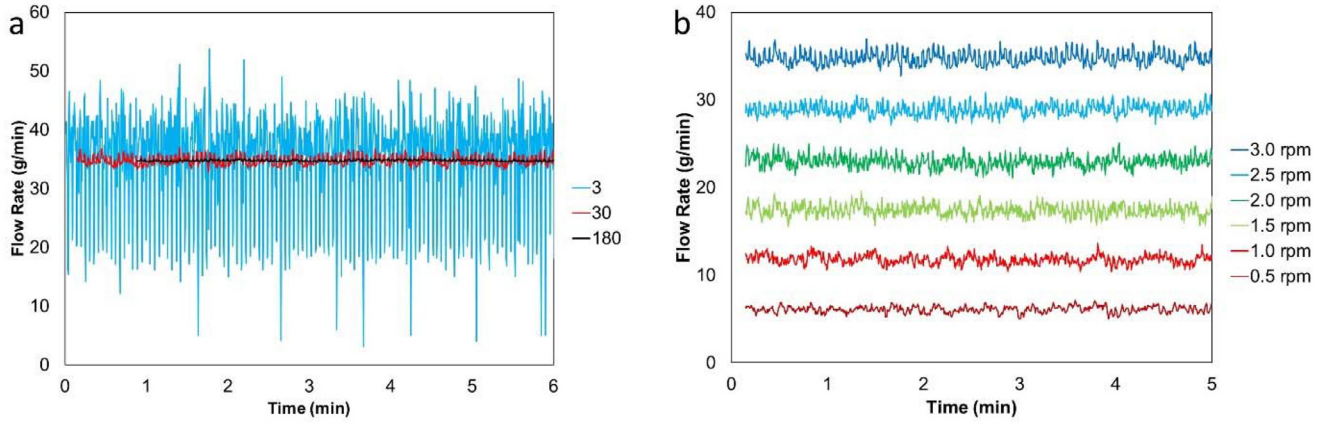


Fig. 3. Water atomised 316 L using high volume scraper. a) Mass flow rate at 3.0 rpm turntable speed, showing moving average window over 3 data points (1 second), 30 data points (10 s) and 180 data points (60 s); b) Moving average window over 30 data points for all turntable speeds.

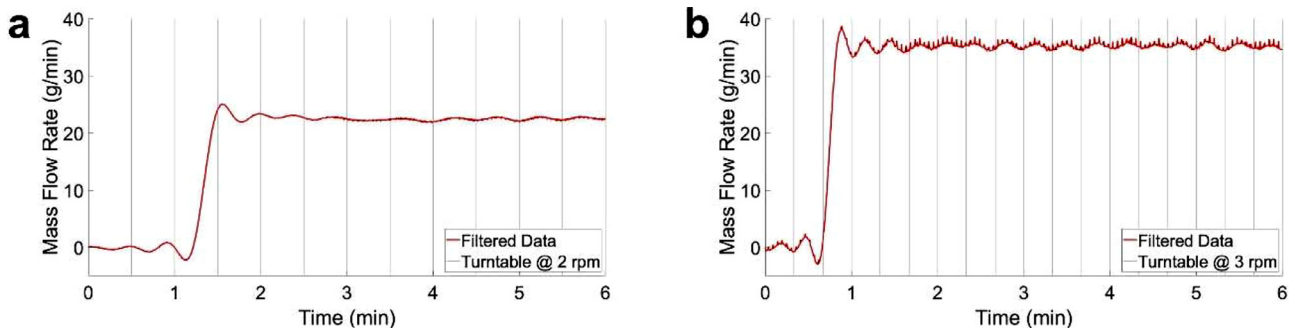


Fig. 4. Mass flow rate for water atomised 316 L using high volume scraper with filtering. a) 2 rpm; b) 3 rpm. Vertical lines indicate the periodicity of the turntable.

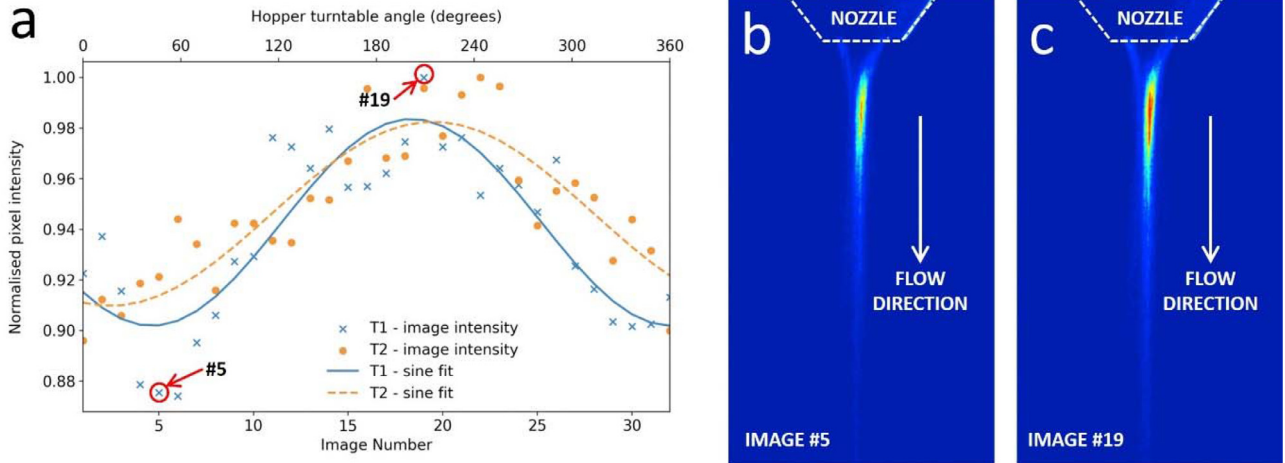


Fig. 5. a) Normalised sum of pixel values over duration of a full turntable rotation at 3.1 rpm, two repeats shown; c) Image #5 from T1; d) Image #19 from T1.

3.3. Constructive & destructive cylinders

Two cylinders were built in GA316 on the 24Vx nozzle, to quantify whether the variation in powder flow rate was of sufficient magnitude to be observed in the physical build. The first cylinder tested for constructive interference, using a circumference matched to the time for one hopper turntable rotation. The second cylinder tested for destructive interference, using a circumference half the size, to confirm that any effects were flow rate driven rather than due to nozzle defects or other external factors.

To achieve a mass flow rate of 16.5 g/min, the hopper was set at 3.1 rpm, taking 19.4 s per rotation. At a deposition speed of 1000 mm/min, this required the first cylinder to have a radius of 51.4 mm, and the second to have a radius of 25.7 mm. If flow variation caused a change in track dimensions it would be magnified over the height of the first cylinder, but would cancel out over the height of the second cylinder.

The larger cylinder showed very uniform behaviour during the build, with no apparent instabilities (Fig. 6). The smaller cylinder had a slight instability around layer 7, which propagated through the remaining layers, causing some ripples on the top edge.

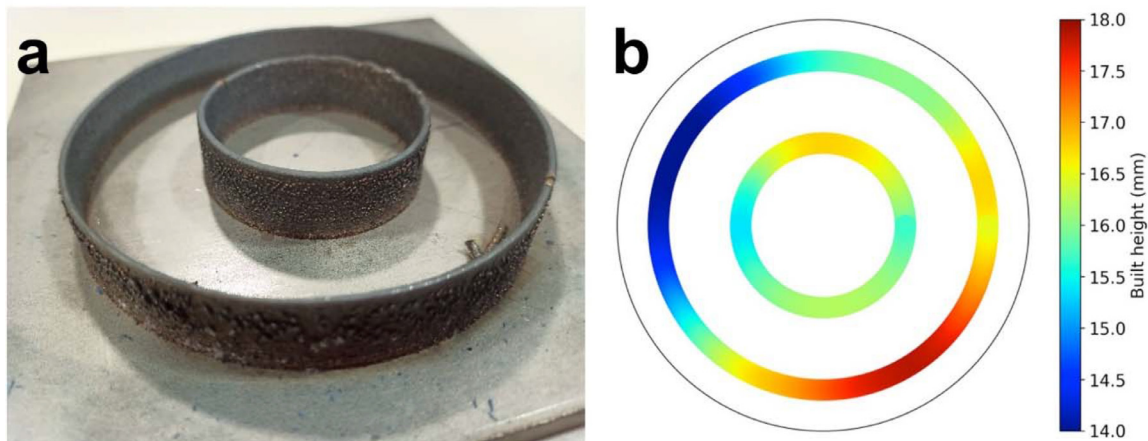


Fig. 6. Cylinders built to test whether turntable-frequency flow variation was observable in the physical build. a) Physical appearance of built cylinders; b) Colour map of cylinder height.

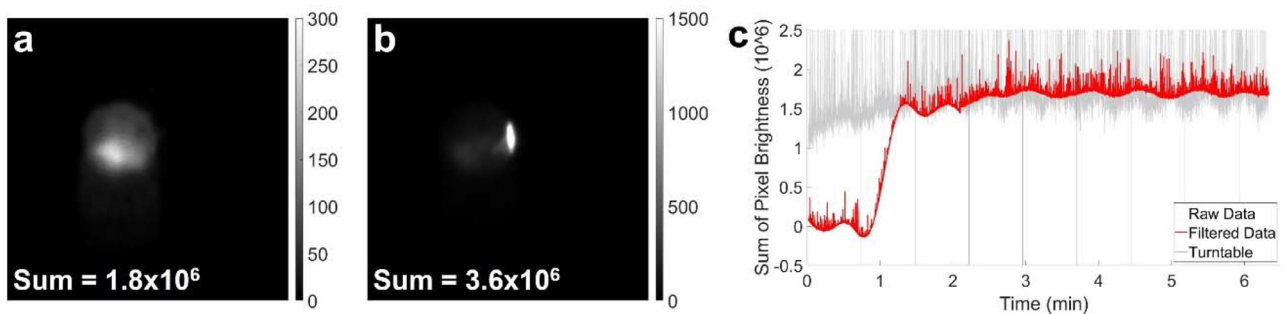


Fig. 7. a) Coaxial image #2249 showing representative melt pool; b) Coaxial image #2248 showing spatter; c) Raw and filtered data of brightness sum showing oscillation at frequency matching hopper turntable rotation, turntable frequency shown for information.

The side view of the large cylinder showed a clear variation in height with circumferential position; trending from 14.0 mm at the lowest point to 17.8 mm at the highest point. The high and low points were directly opposite each other, with a height variation of $\pm 12\%$ of the mean. The smaller cylinder had varied in height from 15.7 mm to 16.7 mm, but with no trends around the circumference.

At 3 rpm, offline measurement showed GA316 to have a mean flow rate of 16.1 g/min with a standard deviation of 3.6 g/min (Table 3). This is greater variation than observed in the built part, which could be related to powder capture efficiency.

3.4. Coaxial imaging cylinders

Cylinders were built with the 10Vx nozzle to assess whether powder mass flow variation would be detectable through coaxial melt pool monitoring and whether it might then influence the use of melt pool imaging for closed-loop control.

The build used a mass flow rate of 7.2 g/min, which required a turntable speed of 1.35 rpm. The coaxial camera was used to capture images of the melt pool. The greyscale values of all pixels in each image were summed, to give a single 'brightness' value for each image [22]. This is not a measurement of melt pool size, but it is expected to show the same general trends as melt pool size within a single build.

Fig. 7a shows a representative melt pool image, with a brightness sum of 1.8×10^6 . Fig. 7b shows an image with spatter, causing a much higher brightness sum of 3.6×10^6 . The grey line in Fig. 7c shows the time series of the raw brightness data through the build; the data is noisy, but there is an oscillating pattern. The raw data was filtered to remove the noise, identifying a clear oscillation at a frequency match-

ing the turntable speed (red line in Fig. 7c), and comparable with that observed in Fig. 2.

4. Discussion

The aim of this work was to investigate the stability of powder flow rates in DED, identify if that variation was of sufficient magnitude to affect the built component, and whether it affected melt pool imaging.

Using offline weight measurement, it was demonstrated that the hopper used in this study produced an oscillating powder flow rate, correlated with the hopper turntable rotation speed (Fig. 2). This was confirmed using side-view imaging, which showed a change in the appearance of the powder stream over a full turntable rotation (Fig. 5).

This was observed for a spherical gas-atomised 316 L powder, commonly used for DED, and a less-spherical water-atomised 316 L powder, which is associated with poorer 'flowability' (Fig. 4). The data was noisier for water-atomised powder, and the amplitude of oscillation was reduced (after noise reduction); this could be related to changes in hopper set-up, fill level and alignment as well as powder type.

The effect on the physical build was assessed using two cylinders, one with the circumference matched to the duration of turntable rotation and one half the size (Fig. 6). The larger cylinder showed constructive interference, the oscillation in flow rate leading to a 12% variation in build height across the top surface. The smaller cylinder had no trend in build height with circumferential position, confirming that the effect was flow rate driven rather than due to external influences.

The final stage was an assessment of coaxial melt pool imaging, collected during a build. The data was noisy, mostly due to spatter creating bright spots, but the filtered signal showed a clear oscillating pattern matching the turntable frequency (Fig. 7).

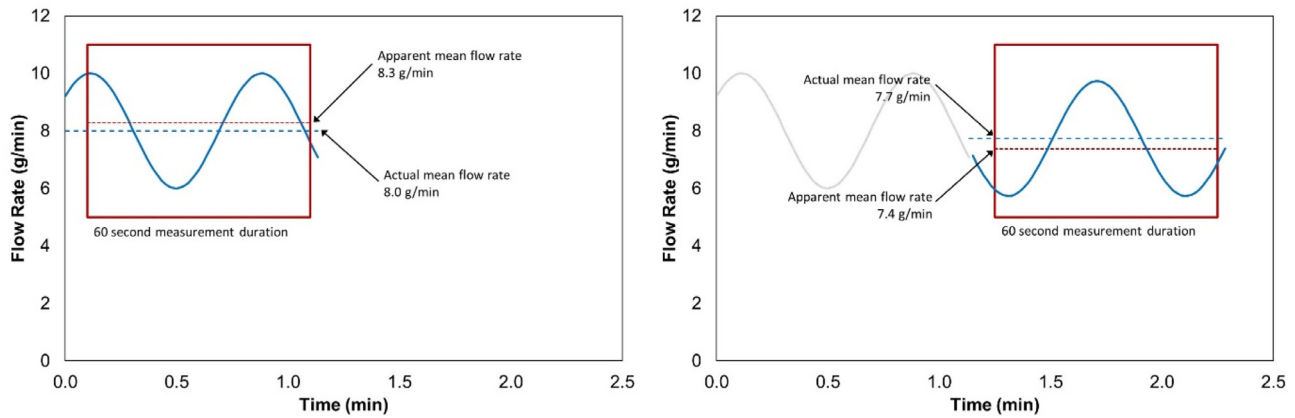


Fig. 8. Schematic interaction between powder flow rate variation and measurement duration. First measurement includes two ‘peaks’ leading to an over-estimate of average flow rate. Turntable speed is then reduced to correct the apparent error. The next measurement includes two ‘troughs’ leading to an under-estimate of average flow rate.

Overall, this work confirmed that DED systems can experience variations in powder flow rate at a magnitude that can affect build quality and that this effect is observable in melt pool imaging. As a single event, flow rate instability will affect melt track height, with the potential to cause defects in the finished component. As a frequent event, this can be magnified through the build depending on the match between the oscillation frequency and the build geometry. This may affect the stand-off distance between the nozzle and the component, leading to a loss of build quality [23,24].

The correlation with turntable rotation speed across different powders, scraper configurations, fill levels and environmental conditions suggests that this is a characteristic of this design of hopper. The hopper construction is complex, so differences in adjustment may influence the noise and magnitude of flow rate variation. The hopper design includes a restriction designed to make the powder at the funnel exit independent of the pressure of stored powder (Fig. 1b), however with dense, free-flowing metal powders, fill level may still have an effect.

To understand if the oscillation can be eliminated, it has been considered in terms of the physical volume of powder involved. For GA316, the powder track on the turntable was nominally 15 mm wide and 0.4 mm high, and running the hopper at 2 rpm produced a mass flow rate of 10.7 ± 1.9 g/min ($\pm 18\%$). This shift in mass flow rate could be caused by a fluctuation of only 70 μ m in track height (the diameter of a single powder particle) or from a combination of much smaller variations in track height, width and rotation speed. This would be difficult to eliminate at source, particularly in a hopper which is manually reassembled after cleaning and has many opportunities for alignment variation.

Variation may also affect the current approach for setting mass flow rate before a build. If measurements are always taken over 60 s, the first measurement could include two ‘peaks’, apparently exceeding the target (Fig. 8). The operator would then adjust the turntable speed down and the next measurement would include two ‘troughs’ apparently falling short of target. This wastes powder and operator time, but can be mitigated by measuring over a complete number of turntable rotations.

A further consideration is how powder flow rate variation could influence image-based closed-loop control approaches [22,25,26]. Fig. 7 shows a variation in the brightness of the melt pool image, correlated with the periodicity of turntable rotation. The effect of flow rate variation on melt pool appearance will depend on a number of factors including the temperature of the particles arriving, how much of the incident laser they scatter, and how much of the monitored light they scatter (the wavelength detected by the imaging system). These may vary between DED systems and even between different powder types, due to the particle time-of-flight from nozzle to melt pool and absorptivity to the different wavelengths. Some potential situations include:

- Drop in flow rate reduces incident laser scattering, allowing more laser energy to reach the melt pool surface causing temperature to increase
- Drop in flow rate reduces in-transit absorption, reducing energy input to the melt pool and causing temperature to decrease
- Drop in flow rate reduces emitted light scattering, allowing more light to reach the camera irrespective of melt pool temperature

A reduction in image brightness will normally be interpreted as a drop in melt pool temperature, and will trigger a control response to increase power and/or reduce deposition speed. If this reduction in brightness has actually been caused by increased powder flow rate scattering the light being emitted from the melt pool, but with no/minimal change in melt pool temperature, then this control response is inappropriate and could result in poor build quality. To achieve an optimised control response, it is therefore beneficial to ensure that flow rate variation is minimised.

Overall, this work highlights the need for closed-loop control of powder flow rate. This would eliminate the need for offline measurement before a build, minimise the risk to build quality from flow rate variation, mitigate against fill level effects as the hopper gradually empties, and ensure that melt pool imaging for temperature monitoring was unaffected by flow rate effects. A ‘hopper-agnostic’ approach would also remove the need for costly root cause analysis and design modifications required to address flow variation at source across different hopper designs.

5. Conclusions

- Powder delivery systems for directed energy deposition processes can exhibit oscillatory variation in mass flow rates, matching the characteristic speed of individual hopper components
- Flow rate variation can be observed at the nozzle exit, both by offline weight measurement and by imaging the powder flow, but may not be identified in pre-build checks measuring over 1–2 min
- Flow rate variation is observed to have a measurable effect on melt track height, with the potential to cause build quality issues
- Melt pool imaging shows a correlating pattern, indicating that flow rate variation can affect melt pool image brightness, and may influence the behaviour of image based control approaches

6. Contributions

Felicity Freeman – Conceptualization, methodology (offline weight measurement, physical builds), software (signal filtering, physical

builds), formal analysis, investigation, writing (original draft), writing (review & editing), visualisation, project administration.

Ben Thomas – Methodology (flow imaging), software (flow imaging), formal analysis, investigation, writing (review & editing).

Lova Chechik – Methodology (coaxial imaging), software (coaxial imaging), writing (review & editing).

Iain Todd – Resources, supervision, funding acquisition.

Declarations of Competing Interest

None

Funding

This work was funded by the Engineering and Physical Sciences Research Council through the Future Manufacturing Hub in Manufacture using Advanced Powder Processes (EP/P006566/1), and by the European Union's Horizon 2020 research and innovation programme under grant agreement No 820776, carried out under FoF-04–2018 project on the topic "Pilot lines on metal additive manufacturing" <http://www.integradeproject.eu/>.

We acknowledge the Henry Royce Institute for Advanced Materials, funded through EPSRC grants EP/R00661X/1, EP/S019367/1, EP/P02470X/1 and EP/P025285/1, for BeAM Magic 2.0 access at The University of Sheffield.

References

- [1] J. Gao, C. Wu, X. Liang, Y. Hao, K. Zhao, Numerical simulation and experimental investigation of the influence of process parameters on gas-powder flow in laser metal deposition, *Opt. Laser Technol.* 125 (2020) 106009, doi:10.1016/j.optlastec.2019.106009.
- [2] S. Takemura, R. Koike, Y. Kakinuma, Y. Sato, Y. Oda, Design of powder nozzle for high resource efficiency in directed energy deposition based on computational fluid dynamics simulation, *Int. J. Adv. Manuf. Technol.* 105 (2019) 4107–4121, doi:10.1007/s00170-019-03552-1.
- [3] K. Shah, et al., Parametric study of development of Inconel-steel functionally graded materials by laser direct metal deposition, *Mater. Des.* 54 (2014) 531–538, doi:10.1016/j.matdes.2013.08.079.
- [4] A.J. Pinkerton, L. Li, Rapid prototyping using direct laser deposition - The effect of powder atomization type and flowrate, *Proc. Inst. Mech. Eng. Part B J. Eng. Manuf.* 217 (2003) 741–752, doi:10.1243/09544050360673134.
- [5] J. Whiting, A. Springer, F. Sciammarella, Real-time acoustic emission monitoring of powder mass flow rate for directed energy deposition, *Addit. Manuf.* 23 (2018) 312–318, doi:10.1016/j.addma.2018.08.015.
- [6] P.P. Breese, T. Hauser, D. Regulin, S. Seebauer, C. Rupprecht, In situ measurement and closed-loop control for powder supply processes Retrofittable solution in the context of laser metal deposition, *Int. J. Adv. Manuf. Technol.* 116 (2021) 889–903, doi:10.1007/s00170-021-07438-z.
- [7] BeAM. *Machine Setup - Magic 2.0*. (2019).
- [8] D. Eisenbarth, P.M. Borges Esteves, F. Wirth, K. Wegener, Spatial powder flow measurement and efficiency prediction for laser direct metal deposition, *Surf. Coatings Technol.* 362 (2019) 397–408, doi:10.1016/j.surfcoat.2019.02.009.
- [9] O.B. Kovalev, A.V. Zaitsev, D. Novichenko, I. Smurov, Theoretical and experimental investigation of gas flows, powder transport and heating in coaxial laser direct metal deposition (DMD) process, *J. Therm. Spray Technol.* 20 (2011) 465–478, doi:10.1007/s11666-010-9539-3.
- [10] P. Balu, P. Leggett, R. Kovacevic, Parametric study on a coaxial multi-material powder flow in laser-based powder deposition process, *J. Mater. Process. Technol.* 212 (2012) 1598–1610, doi:10.1016/j.jmatprotec.2012.02.020.
- [11] V. Kovalenko, et al., Development of Multichannel Gas-powder Feeding System Coaxial with Laser Beam, *Procedia CIRP* 42 (2016) 96–100, doi:10.1016/j.procir.2016.02.197.
- [12] Fraunhofer Institute for Material and Beam Technology IWS. *LIsec – System integrated powder nozzle measuring system for additive manufacturing applications*. https://www.iws.fraunhofer.de/content/dam/iws/en/documents/publications/product_sheets/600-10_pulverduesenmesssystem_en.pdf.
- [13] Oerlikon. *Product Data Sheet Single 220 Series Gravimetric Powder Feeder*. <https://www.oerlikon.com/metco/en/media-resources/download-center/>, (2021).
- [14] M. Ansari, A. Mohamadizadeh, Y. Huang, V. Paserin, E. Toyserkani, Laser directed energy deposition of water-atomized iron powder: process optimization and microstructure of single-tracks, *Opt. Laser Technol.* 112 (2019) 485–493, doi:10.1016/j.optlastec.2018.11.054.
- [15] L. Chechik, et al., Variation of texture anisotropy and hardness with build parameters and wall height in directed-energy-deposited 316L steel, *Addit. Manuf.* 38 (2020) 101806, doi:10.1016/j.addma.2020.101806.
- [16] A. Alhuzaim, S. Imbrogno, M.M. Attallah, Controlling microstructural and mechanical properties of direct laser deposited Inconel 718 via laser power, *J. Alloys Compd.* 872 (2021) 159588, doi:10.1016/j.jallcom.2021.159588.
- [17] Sandmeyer Steel. *Specification Sheet: alloy 316/316 L. 3* <https://www.sandmeyersteel.com/images/316-316L-317L-Spec-Sheet.pdf>, (2014).
- [18] R. Sampson, et al., An improved methodology of melt pool monitoring of direct energy deposition processes, *Opt. Laser Technol.* 127 (2020) 106194, doi:10.1016/j.optlastec.2020.106194.
- [19] Scott, J., Gupta, N., Weber, C. & Caffrey, T. *Additive Manufacturing: status and Opportunities*. https://cgsr.llnl.gov/content/assets/docs/IDA/AdditiveM3D_33012_Final.pdf (2012).
- [20] Measurement Science Roadmap For Metal-Based Additive Manufacturing, National Institute of Standards and Technology., 2013. https://www.nist.gov/system/files/documents/el/isd/NISTAdd_Mfg_Report_FINAL-2.pdf
- [21] K. Kassym, A. Perveen, Atomization processes of metal powders for 3D printing, *Mater. Today Proc.* 26 (2019) 1727–1733, doi:10.1016/j.matpr.2020.02.364.
- [22] S. Baraldo, A. Vandone, A. Valente, E. Carpanzano, Closed-loop control by laser power modulation in direct energy deposition additive manufacturing, *Lecture Notes Mech. Eng.* (2020), doi:10.1007/978-3-030-46212-3_9 10.1007/978-3-030-46212-3_9.
- [23] S. Donadello, M. Motta, A.G. Demir, B. Previtali, Monitoring of laser metal deposition height by means of coaxial laser triangulation, *Opt. Lasers Eng.* 112 (2018) 136–144, doi:10.1016/j.optlaseng.2018.09.012.
- [24] J.C. Haley, et al., Working distance passive stability in laser directed energy deposition additive manufacturing, *Mater. Des.* 161 (2019) 86–94, doi:10.1016/j.matdes.2018.11.021.
- [25] M. Akbari, R. Kovacevic, Closed loop control of melt pool width in robotized laser powder-directed energy deposition process, *Int. J. Adv. Manuf. Technol.* 104 (2019) 2887–2898, doi:10.1007/s00170-019-04195-y.
- [26] C.W.B. Group. *Welding Industry Day: closed-Loop Feedback Control for Industrial DED*. <https://www.youtube.com/watch?v=dyG7VWWpXZg>, (2020).